LA-UR- 92-1302

Title: **Problems in Neutrino Electron Scattering with 1-GeV Neutrinos**

LA-UR--92-1302

DE92 013535

Author(s): *D. Hywel White, MP-4*

Submitted to: *The TRIUMF Neutrino Workshop,*
Lake Louise, Alberta, Canada, February 18-21, 1992

Los Alamos
NATIONAL LABORATORY

Problems in Neutrino Electron Scattering with 1-GeV Neutrinos

D. Hywel White, MP-4, LAMPF

Introduction

Neutrino physics has often been limited by lack of events. This limitation has been not so much for events in total, but for events in selected channels. The basic strategy for dealing with this issue has been to build massive detectors in which target and event detection have been combined. This strategy has been very successful, but it does carry the difficulty that, given a large detector mass, financial limitations apply to the detail with which events may be detected and reconstructed. At KAON some of these difficulties will be alleviated by the increase in neutrino flux, which may make the construction of smaller and more specialized detectors feasible. At the Lake Louise workshop a great deal of interest was expressed in neutrino electron scattering; we shall describe here the limitations of the BNL detector as they emerged in the measurement of $\sin^2\theta_w$ at BNL. In this context the knowledge of the beam was an intrinsic part of the experimental systematic errors, and we start with a description of the beam.

Neutrino Beam

The neutrino beam that was used by the BNL collaboration is described in a paper that is reproduced here as an appendix [1]. Protons from the BNL AGS at 28.5 GeV produced secondary particles in a titanium target about two interaction lengths long. This is worth mentioning only because the target was sapphire at the start of the experiment, which has the desirable high density and low Z. After some time the AGS began to run above 1×10^{13} protons per pulse, the target then was reduced to a noxious and highly radioactive black powder that did little for particle production. This beam used two horns to focus the charged particles, as described in [1]. The central momentum was 3 GeV/c and for much of the experiment the decay region was 50 m long. The magnetic focusing system was designed to transform the particles from an extended target to parallel beam down the decay tunnel The biggest gain of the horn system comes from increasing the momentum spread for which particles are contained in the decay region. If the beam is indeed parallel and the detector is at the end of the shield, then a simple theorem exists stating that the decay region should be double the shield thickness for optimum flux at the detector. This is about 0.28 of a decay length at 3 GeV/c. Both charged pions and kaons are focused and the predominant source of ν_μ came from the $(\mu + \nu_\mu)$ final state in each case. In Fig. 1 (Fig. 12 of [1]) is shown the calculated distribution of ν_μ momentum for there two particles. In Fig. 2 (Fig. 8 of the same paper) is shown the sum distribution together with the measured spectrum.

This spectrum was deduced by measuring the reaction

$$\nu_\mu + n \rightarrow \mu^- + p$$

(or the antineutrino equivalent).

program NUBEAM, which incorporates all known branching modes of K and π and uses a reasonably economical scheme to transport particles through the beam hardware. The principal input data is then the particle production spectra that were obtained initially from the atlas of particle production [2]. These particle production data are for thin targets and the principal uncertainty in the actual particle production comes from the thick target that was used. These production data were modified to fit the neutrino spectrum, and it was then verified that the shape of other spectra were reproduced. This is discussed further below. In our opinion this hadron shower simulation in the production target is one of the more vexing issues facing a more precise simulation of this neutrino flux. The contamination of opposite helicity neutrinos is a delicate calculation that is a fairly severe test of the simulation. The combination of spectra for both polarities of focusing and the wrong helicity contamination are a constrained set of data. Opposite helicity neutrinos are apparent from the sign of the muon in quasi-elastic events so that their spectrum as a function of energy is also available subject to the same difficulties as in determining the majority spectrum. In [1], modified particle production spectra for 30 GeV/c are shown.

To compute the ν_e in the beam, other branching modes become important ($K \rightarrow \pi^0 + e + \nu_e$, $\pi - \mu - e$) as well as production from K_L, which decay downstream of the horn system. At high energy, the neutrino spectrum becomes contaminated by ν_e from K decay to a much greater extent than at low energies. This limits the energy range of the recoil electrons for which it makes sense to use in the fit. Moreover, the high energy neutrinos produce low-energy recoil electrons from the low end of the y distribution so that a good knowledge of the high-energy end of the spectrum is needed, especially after allowing for weighting of the cross section by neutrino energy. It is useful to remember that the neutrino and antineutrino energy distributions are significantly different as a function of energy.

At the low-energy end of the spectrum is where the most severe problems arise. First the muons at low neutrino energies are emitted at large angles and so the acceptance of the spectrometer decreases along with the cross section. Furthermore, the contamination from charged pions produced in inelastic reactions rises rapidly as the energy decreases. Pions are very hard to tell from muons below 1 GeV. Pion decay is not much of a handle, and the range is such that few of them interact. The reason that data points do not extend much below 1 GeV is that the pion contamination becomes very severe. If this were not enough, ν_e contamination is also running away because of $\pi - \mu - e$ multiple decay making ν_e in the beam. The extent of this problem can be understood in the low energy limit where the ratio of ν_e to ν_μ approaches 50%, not 1%, which is the value where muon flux is maximal. This concern with the low-energy behavior of neutrino flux has an effect at low recoil electron energies, and even more so in antineutrino electron scattering. In the BNL experiment this asymmetry was important. In fact, almost any experiment that will claim precision in $\sin^2\theta_w$ will use a comparison of neutrino to antineutrino scattering in some way.

The BNL Detector

The detector is shown schematically in Fig. 4 (Fig. 2 of [3]) and on a larger scale in Fig. 3 (Fig. 1 of [3]). The second appendix is a *NIM* article that was written on the BNL detector. The goal of the detector design was to make the device as fully active as possible;

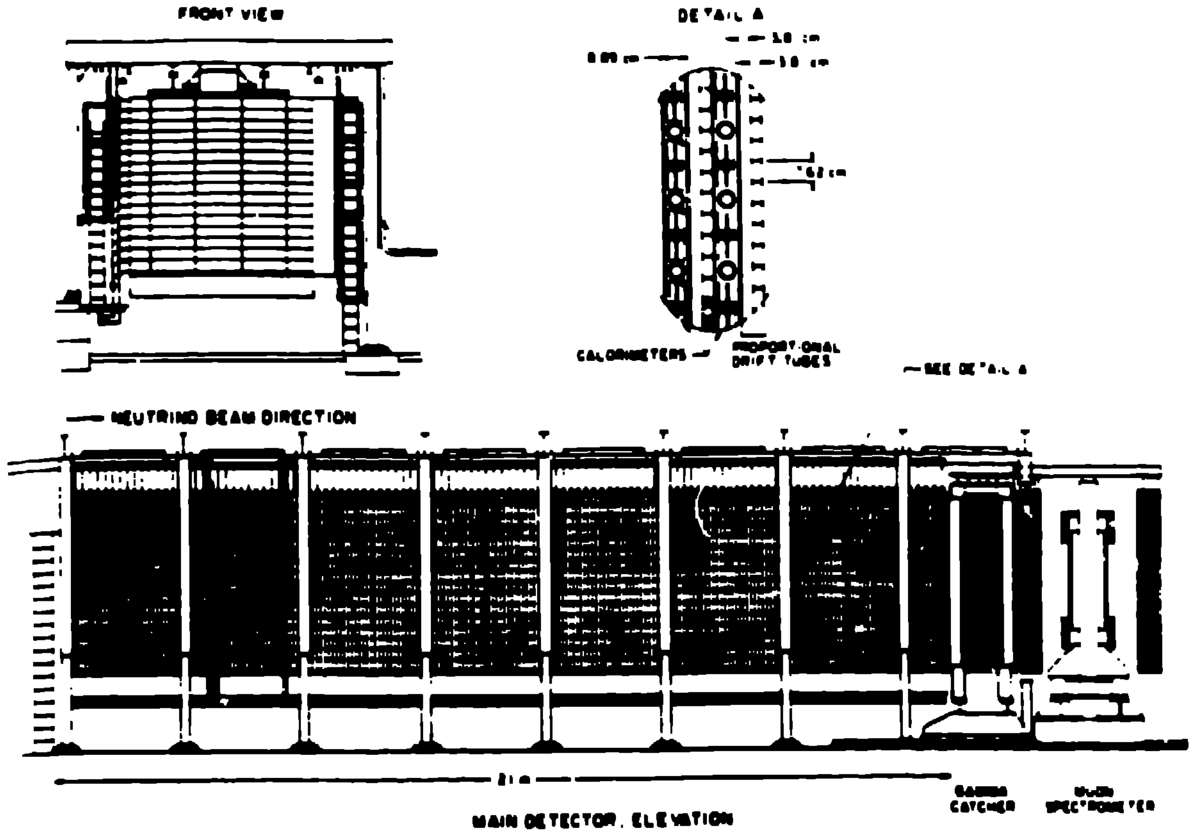

Fig. 4. Schematic drawing of the complete BNL-Brown-KEK-Osaka-Pennsylvania-Stony Brook neutrino device.

in fact, nearly 90% was achieved. This property will be discussed in more detail below. The main part of the detector consisted of two components, the calorimeter and the proportional drift tubes. The calorimeter cell consisted of a lucite box 25 cm × 8.9 cm × 4 m. Light was totally internally reflected, and detected by a phototube on each end. The time of the energy deposit was measured to about one nanosecond, and position along the tube was measured to a few cm. The energy resolution of the detector (0.13 / $\sqrt{E_e}$ for electrons) is dominated by energy deposit in the calorimeter. The position of charged tracks was determined by the proportional drift tubes which recorded time and pulse height. Time was translated into position good to about 1 mm. The primary limitation on position resolution was the multiple scattering in the calorimeter material. Angular resolution (16 mr / $\sqrt{E}$) was of primary interest in the electron scattering experiment, initially to produce good signal to background in the forward peak. Eventually, the shape of the angular distribution became important increasing the interest in the angular resolution.

The energy and angular resolutions were close to that expected because they were dominated by the physical properties of the detector more than the detailed performance of some of the individual elements. One property that depended on the detailed performance was photon to electron separation. Photons essentially convert to electron pairs at these energies (200-2100 MeV) so the energy deposited in the calorimeters (dE/dx) and in the gas of the PDTs was typically twice that for electrons and gave separation between electrons and photons which was very important. The dE/dx rejection is shown in Fig. 5 (Fig. 18 of [3]). However this technique became less powerful below 200 MeV in the region where photon contamination was strongest. Typically neutral current reactions like

$$\nu_\mu + n \rightarrow \nu_\mu + \pi^0 + n$$

give two gamma rays one of which is lost in the detector. Although losing a photon is relatively rare, the cross section above is about one thousand times that of neutrino electron scattering. The free space represented by the gas of the PDTs is a definite problem; in fact, this is only part of the problem that the lateral density for particle detection for both photon and neutron is too low. A sample of photons was obtained by looking for evidence of other activity upstream in the detector in time with the photon and this was very effective in establishing the shape of the single photon spectrum.

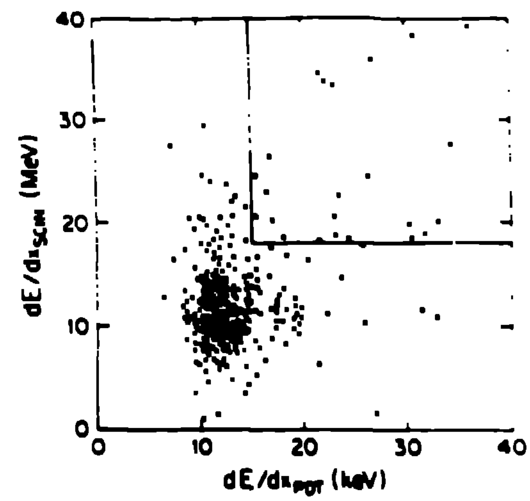

Fig. 5. A scatter plot of the energy deposited in the first scintillator cell past the vertex cell ($(dE/dx)_{SCIN}$) vs a truncated mean of the energy deposits in the second and third PDT planes past the vertex cell ($(dE/dx)_{PDT}$) for test beam electron. Events valling in the box in the upper right corner would initially be recognized as photons.

It is our conviction that the use of the ratio of neutrino to antineutrino cross sections measured separately to measure $\sin^2\theta_w$ cannot be pushed to the level below 1% precision. Many systematic errors come in, and even though the performance of the detector can be improved by making it less dense, and making it fully sensitive there seems to be hard limits before the sub 1% regime is accessible. A possibility in our opinion is to concentrate on the difference in the angular distributions for neutrino and antineutrino scattering as was done in the BNL experiment [4].

In any case, the understanding of the beam and the detector performance must be adequate to resolve components of the background which varies little in angular distribution. In the BNL experiment it had three distinct components, which ended up in comparable quantities in the data. Electrons are identified by removing all of the clear tracks and those that are left are electron candidates; a typical electron event is shown in Fig. 6 (Fig. 17 of [3]). Photons are eliminated by the dE/dx cut set so that 90% of electrons are retained, but some single photons remain in the sample. Pions occasionally interact in the upstream part of the event and look badly enough so as to be retained as electrons. Finally ν_e induced quasi-elastic events at low Q^2 belong in the data set and have the unfortunate property that at small Q^2 Pauli suppression makes the cross section diminish. A straight extrapolation will give an error on the extraction of the neutrino electron scattering signal. The quasi-elastic cross section at zero Q^2 is the same for neutrinos and antineutrinos, but everything else is different. The final statement is that achieving precision in neutrino electron scattering is difficult; events are not enough. We counsel careful attention to many of these details before committing to a particular approach.

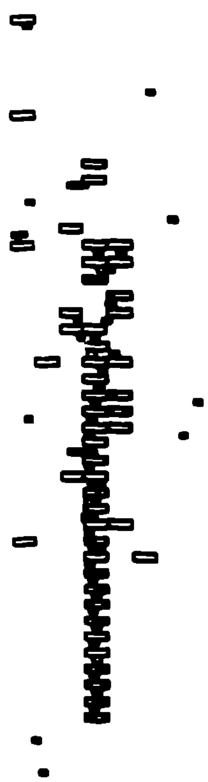

Fig. 6. A side view of a typical electromagnetic shower in the detector. The large rectangles represent scintillator cells and the smaller rectangles PDT cells hit. Approximately five modules comprise one radiation length.

References

1. L. A. Ahrens, S. H. Aronson, P. L. Connolly, B. G. Gibbard, M. J. Murtagh, S. J. Murtagh et al., "Determination of Fluxes in the Brookhaven Wide-Band Beams," *Physical Review D1* **34**, 75 (1986), Appendix [1].
2. H. Grote, R. Hagedorn, and J. Ranft, CERN Report 1970 (unpublished).
3. L. A. Ahrens, S. H. Aronson, P. L. Connolly, T. Erickson, B. G. Gibbard, M. J. Murtagh et al., "A Massive Fine-Grained Detector For The Elastic Reactions Induced By Neutrinos in the GeV Energy Region," *Nucl. Instrum. Methods A* **254**, 515-528 (1987), Appendix [2].
4. L. A. Ahrens, S. H. Aronson, P. L. Connolly, B. G. Gibbard, M. J. Murtagh, S. J. Murtagh et al., "Determination of Electroweak Parameters from the Elastic Scattering of Muon Neutrinos and Antineutrinos on Electrons," *Phys. Rev. D* **41**, 3297 (1990), Appendix [3].